

Analyzing the magnetic influence on magneto-optical interactions

Francisco Estrada¹ and José Holanda^{2,*}

¹*Facultad de Biología, Universidad Michoacana de San Nicolas de Hidalgo, Av. F. J. Mujica s/n Cd. Universitaria, Morelia, Michoacán, México.*

²*Programa de Pós-Graduação em Engenharia Física, Universidade Federal Rural de Pernambuco, 54518-430, Cabo de Santo Agostinho, Pernambuco, Brazil.*

Abstract

Here, we study the magneto-optical interactions in magnetic structures considering the dependence of the interactions with the magnetic field. We perform numerical simulations in a structure of magnetic nanowires, considering them as one chain of strongly interacting single-domain particles. Robustly, we obtain a quantitative value for the interactions, which allows us to classify them into two magnetic states: demagnetized and magnetized.

Keywords: Magneto-optical, magnetic states, interacting system, energy balance

1. Introduction

The recent interest of the scientific community in magneto-optical interactions has opened the possibility of a global understanding of characteristics not yet dazdled in nanomaterials [1-6]. Minimizing the bit size in one magneto-optical system for data recording is a challenge for optoelectronics and spintronics applications [3-14]. Such reduction produces an increase in the interactions

*Corresponding author: joseholanda.silvajunior@ufrpe.br

between components of the structure. The scientific interest actual is the quantification (codification) of these interactions. One of the systems that have a high particle distribution density is the arrays of magnetic nanowires electrodeposited in alumina membranes [6, 8-14]. This type of system can present different magnetization reversal modes with a predominant coherent configuration [2, 8-20]. Such systems can be strongly influenced by magneto-optical interactions [2-21]. The influence is detected mainly during the magnetization process with light, which always presents reversible and irreversible components. Furthermore, a striking feature of the magnetization process is that it is not possible to separate the parts of their hysteresis without losing information due to changes in the magnetic energies of the structure. This means that many properties remain hidden during the magnetization process and there is a need for understanding. The study from the magneto-optical interactions can be performed using the remanent state obtained during the magnetization process [2].

In a particular system, the well-established normalized Δm curves (Δm_N) produce results of the interaction effects, such curves are comparisons between isothermal remanent magnetization ($IRM(H)$) and direct current demagnetization ($DCD(H)$) curves, which define other physical quantities such as $m_d(H) = DCD(H)/IRM(H_{Max})$ and $m_r(H) = IRM(H)/IRM(H_{Max})$ that are normalized considering the value obtained with maximum magnetic field [2, 17, 18, 22-27]. In this paper we present a numerical study on the predominant magneto-optical interactions in structures, for that, we perform numerical simulations in a system of magnetic nanowires, considering them as one chain of strongly interacting single-domain particles. After analyzing magneto-optical interactions, we observe two types of magnetic states, i. e., magnetized and demagnetized, which reveal the main characteristics of magneto-optical energies. Our approach seeks to describe the light-matter interaction with the application of a magnetic field, where the light only serves to excite the magneto-optical effects, that is, all results are obtained considering the dependence of magneto-optical interactions with the magnetic field.

2. Continuous approach

The effects of the magnetic interactions in structures have been studied by using Δm curves [17, 18, 22-29] or discrete models without analyzing the dependence directly on the magnetic field and light [2]. The Δm curves are obtained through the relationships between the $m_d(H)$ and $m_r(H)$ curves, where the initial magnetic state of the structure differentiates them. The model proposed by Stoner Wohlfarth [17, 27] reveals an intrinsic relationship between $m_d(H)$ and $m_r(H)$ for non-interacting structures. Based on this fact, we propose here that the magneto-optical interactions for non-interacting particles have one associated intensity that can be written as

$$I_{N-I} = \left| \int_{H_i}^{H_f} \left(\frac{\eta_{N-I}}{\Delta H} \right) dH \right|, \quad (1)$$

where $H_f > H_i$ and $\eta_{N-I} = [1 - 2m_r(H)] - m_d(H)$. The magnetic fields H_f and H_i represent the maximum and minimum fields in the interval $\Delta H = H_f - H_i$, respectively. In most experimental systems, the minimum magnetic field H_i is zero. To better describe real systems, Henkel postulated that the difference in this behavior in a simple design was due to the interactions between the part of the structure. Usually, in experimental measurements, the data are far from the curve obtained with equation (1) [17, 18, 22-29]. Thus, equation (1) considers that the magnetization and demagnetization processes are the same. Qualitatively, the type of interaction was defined by inserting a term Δm in equation (1). Based on this, we propose here that the intensity of the magneto-optical interactions for interacting particles can be written

$$I_I = \left| \int_{H_i}^{H_f} \left(\frac{\eta_I}{\Delta H} \right) dH \right|, \quad (2)$$

where $\eta_I = \Delta m_N + [1 - 2m_r(H)] - m_d(H)$. The indices $N - I$ and I in equations (1) and (2) are associated with η for systems without and with interactions. When the predominant magneto-optical interactions are demagnetizing (PMOID), $\Delta m_N < 0$; and when the predominant magneto-optical interactions are magnetizing (PMOIM), $\Delta m_N > 0$. The methodology presented here for

the calculation from the magneto-optical interactions uses equations (1) and (2) resulting in a numerical value for the magneto-optical interactions of the structure. Hence, the intensity value from the magneto-optical interactions is obtained through Eqs. (1) and (2) by

$$I = \left| \int_{H_i}^{H_f} \left(\frac{\Delta m_N}{\Delta H} \right) dH \right|. \quad (3)$$

Equation (3) represents both PMOID and PMOIM interactions so that we can rewrite it as

$$I_k = \left| \int_{H_i}^{H_f} \left(\frac{\Delta m_N}{\Delta H} \right) dH \right| \rightarrow \begin{cases} \Delta m_N = \Delta m^D / |\Delta m_{Max}^D| < 0 & \text{for PMOID,} \\ \Delta m_N = \Delta m^M / |\Delta m_{Max}^M| > 0 & \text{for PMOIM.} \end{cases} \quad (4)$$

where $k = \text{PMOID}$ ($\Delta m_N < 0$) or PMOIM ($\Delta m_N > 0$).

3. Results and discussion

Our results were obtained considering a nanowire as one chain of interacting ellipsoidal grains according to Figure 1. Experimentally, the length of the grains

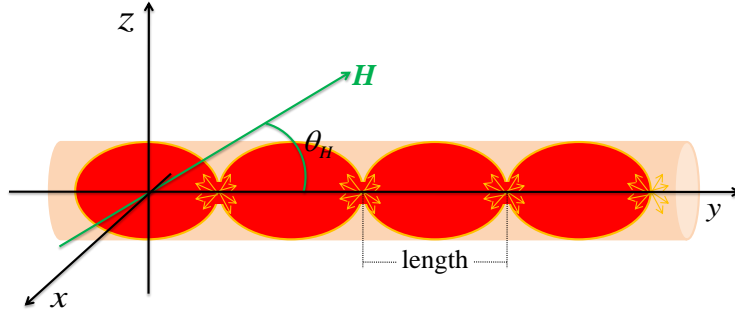


Figure 1: (Color online) Schematic of a nanowire (length much larger than the diameter) as one chain of interacting single-domain particles, which are ellipsoidal grains.

is on the order of 20 to 100 nm, as in single-domain particles [3-14]. Demagnetizing interactions are obtained frequently in experimental measurements [17,

18, 22-29], this is due to, in most cases, the magnetic response of structures being contrary to the applied magnetic field H , leaving the system in a global demagnetized state. Usually, the dependence of Δm_N in terms of applied magnetic field H on systems involving PMOID behavior is $\Delta m^D / |\Delta m_{Max}^D|$, where $\Delta m^D = -(H_C^D)^2 / [(H - H_C^D)^2 + (\Delta J_D)^2]$, H_C^D is the critical demagnetizing field (for $|\Delta m^D|$ maximum, i.e., for $|\Delta m_{Max}^D|$) and ΔJ_D is the demagnetizing linewidth. For all our calculations, we considered $\Delta J_D = 1\% H_C^D$. We did this to condense the energy balance of the magneto-optical interactions so that they would produce a kind of avalanche. Figure 2 shows the interactions (Regions I) considering the Δm_N curves obtained with $H_C^D = 0.75$ kOe (Figure 2(a)), $H_C^D = 2.5$ kOe (Figure 2(b)), $H_C^D = 5.0$ kOe (Figure 2(c)) and $H_C^D = 7.5$ kOe (Figure 2(d)), which are defined as interaction maps. The intensities values of the

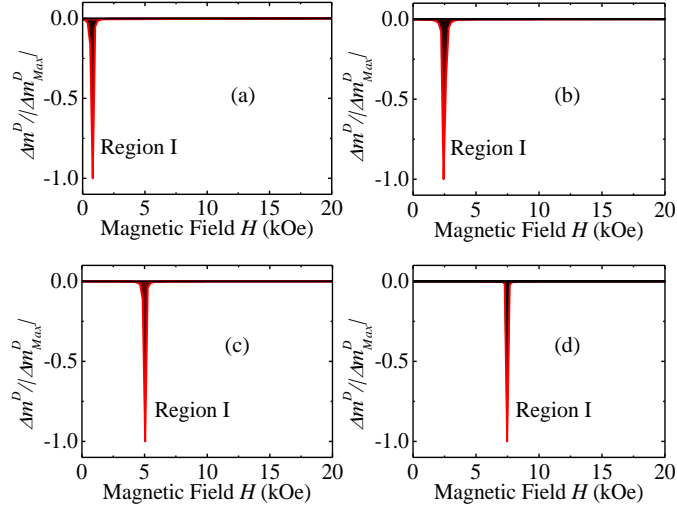


Figure 2: (Color online) Interaction maps calculated from the magneto-optical interactions in terms of the applied magnetic field to different critical demagnetizing field H_C^D . (a) $H_C^D = 0.75$ kOe, (b) $H_C^D = 2.5$ kOe, (c) $H_C^D = 5.0$ kOe and (d) $H_C^D = 7.5$ kOe. The interaction maps were results obtained with the equations (1) and (2), and the intensities were calculated using the equation (4), which are $I_{PMOID} = 0.26$ (item a), $I_{PMOID} = 0.32$ (item b), $I_{PMOID} = 0.25$ (item c), and $I_{PMOID} = 0.21$ (item d).

interactions were numerically calculated using the Eq. (4), which are $I_{PMOIM} = 0.26, 0.32, 0.25,$ and $0.21,$ for Figures 2 (a), (b), (c), and (d), respectively. In this system, the magnetic behavior can often create magnetizing effects due to the exchange interactions of the structure, which are extremely important for the excitation of spin waves [30-34]. Such exchange interactions arise due to defects between grains that cause propagation of domain walls (see insert of Figure 3(a)).

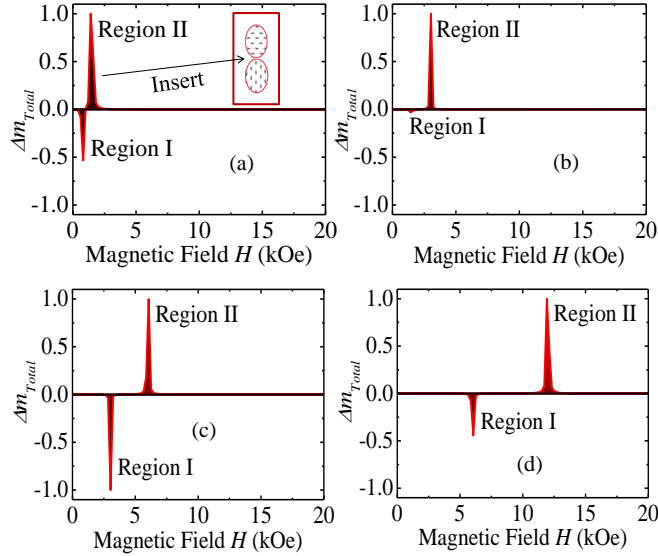


Figure 3: (Color online) Interaction maps calculated from the magnetic interactions in terms of the applied magnetic field to different critical fields demagnetizing H_C^D and magnetizing H_C^M . (a) $H_C^D = 0.75$ kOe and $H_C^M = 1.5$ kOe, (b) $H_C^D = 1.5$ kOe and $H_C^M = 3.0$ kOe, (c) $H_C^D = 3.0$ kOe and $H_C^M = 6.0$ kOe, and (d) $H_C^D = 6.0$ kOe and $H_C^M = 12$ kOe. The interaction maps were results determined with the equations (1) and (2), and the intensities were calculated using the equation (4), which are for the PMOIM interactions, $I_{PMOIM} = 0.12$ (item a), $I_{PMOIM} = 0.01$ (item b), $I_{PMOIM} = 0.21$ (item c), and $I_{PMOIM} = 0.12$ (item d) and for PMOIM interactions, $I_{PMOIM} = 0.35$ (item a), $I_{PMOIM} = 0.21$ (item b), $I_{PMOIM} = 0.27$ (item c), and $I_{PMOIM} = 0.35$ (item d).

According to the spin-wave theory [30, 31], effects that produce exchange

interactions are relevant for their study and understanding. The proposal that we present can analyze the global knowledge of such results. To analyze the possible PMOID behavior, we consider the effects that describe them (PMOID and PMOIM) as, $\Delta m_{Total} = \Delta m^D / |\Delta m_{Max}^D| + \Delta m^M / |\Delta m_{Max}^M|$, where $\Delta m^D = -(H_C^D)^2 / [(H - H_C^D)^2 + (\Delta J_D)^2]$ and $\Delta m^M = (H_C^M)^2 / [(H - H_C^M)^2 + (\Delta J_M)^2]$, which can also describe very well experimental measurements obtained in the laboratory [17, 18, 22-29]. Here, ΔJ_M is the magnetizing linewidth, in which we consider $\Delta J_M = 1\% H_C^M$ for all calculations. Figures 3 (a), (b), (c), and (d) show the PMOID behavior (Regions I) for the different $\Delta m^D / |\Delta m_{Max}^D|$ curves obtained with critical magnetic fields of $H_C^D = 0.75$ kOe, $H_C^D = 1.5$ kOe, $H_C^D = 3.0$ kOe, and $H_C^D = 6.0$ kOe, respectively. The same Figures 3 (a), (b), (c), and (d) also show the PMOIM behavior (Regions II) for the different $\Delta m^M / |\Delta m_{Max}^M|$ curves obtained with critical fields of $H_C^M = 1.5$ kOe, $H_C^M = 3.0$ kOe, $H_C^M = 6.0$ kOe, and $H_C^M = 12$ kOe, respectively. As results obtained with the calculation of PMOID and PMOIM interaction maps of Figure 3 using the Eq. (4), we bring the values, $I_{PMOID} = 0.12, 0.01, 0.21,$ and 0.12 for PMOID interactions, and $I_{PMOIM} = 0.35, 0.21, 0.27,$ and 0.35 for PMOIM interactions, which are shown in Table 1.

Table 1: Shows the intensity values of interactions (PMOID and PMOIM) obtained from the interaction maps of Figure 3.

H_C^D (kOe)	H_C^M (kOe)	I_{PMOID}	I_{PMOIM}
0.75	1.5	0.12	0.35
1.5	3.0	0.01	0.21
3.0	6.0	0.21	0.27
6.0	12	0.12	0.35

The demagnetizing and magnetizing effects are results of the energy balance due to the magnetization process as also shown in Table 1. To understand the angular behavior of magneto-optical interactions in a strongly interacting sys-

tem, we present in Figure 4 the angular dependence from the interactions con-

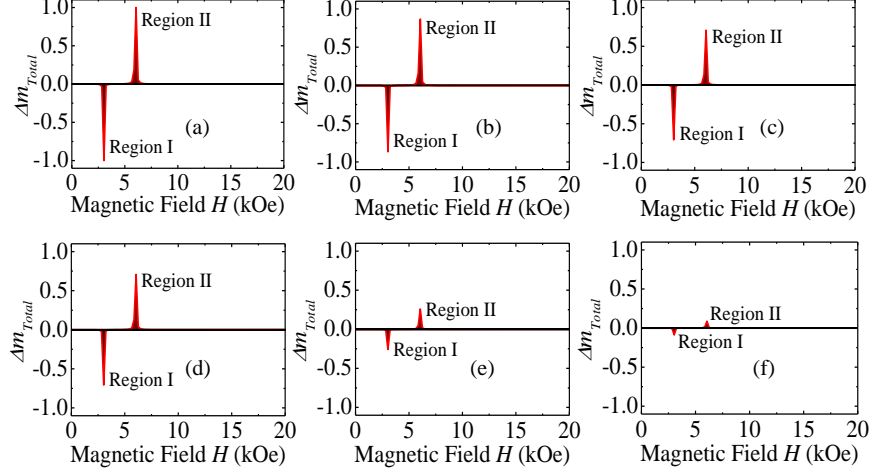


Figure 4: (Color online) Angular dependence of magneto-optical interactions for different angles. The interaction maps were results obtained with the equations (1), (2), and $\Delta m_{Total} = (\Delta m^D/|\Delta m_{Max}^D| + \Delta m^M/|\Delta m_{Max}^M|) \cos(\theta_H)$ to $H_C^D = 3$ kOe and $H_C^M = 6$ kOe. (a) $\theta_H = 0^\circ$, (b) $\theta_H = 30^\circ$, (c) $\theta_H = 45^\circ$, (d) $\theta_H = 60^\circ$, (e) $\theta_H = 75^\circ$ and (f) $\theta_H = 85^\circ$.

sidering the relation $\Delta m_{Total} = (\Delta m^D/|\Delta m_{Max}^D| + \Delta m^M/|\Delta m_{Max}^M|) \cos(\theta_H)$ [2, 8, 13, 16, 29] to $H_C^D = 3$ kOe and $H_C^M = 6$ kOe. This approach describes in detail the behavior of magneto-optical interactions in a magnetic nanowire modeled as a chain of interacting ellipsoidal grains [8, 25-28]. Such dependence shows that for a magnetic field applied parallel to the wire axis, the PMOIM and PMOID behaviors are maximum and decrease with increasing angle θ_H . This behavior is result of the decrease in interactions between the grains as the magnetic field becomes perpendicular to the wire axis. In Figure 5 we show the general variation of the intensity values from the magneto-optical interactions (I_{PMOIM} and I_{PMOID}) as a function of the angle θ_H , where we use $\Delta m_{Total} = (\Delta m^D/|\Delta m_{Max}^D| + \Delta m^M/|\Delta m_{Max}^M|) \cos(\theta_H)$ with $H_C^D = 3$ kOe, $\Delta J_D = 1\%H_C^D$, $H_C^M = 6$ kOe and $\Delta J_M = 1\%H_C^M$. We define for any wave-

length the best conditions to observe the maximum number of magneto-optical interactions. We also observed that it is possible increase the intensity of interactions when the PMIOD and PMOIM effects have similar intensities.

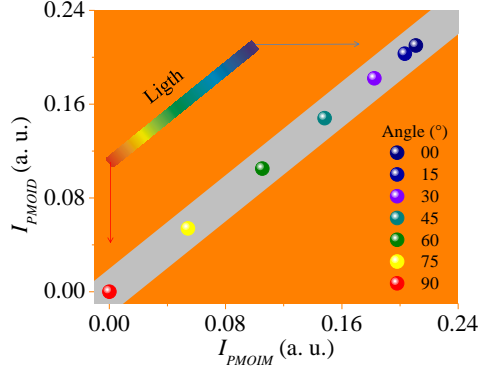


Figure 5: (Color online) Magneto-optical interactions (I_{PMOID} and I_{PMOIM}) as a function of the angle θ_H , where we use $\Delta m_{Total} = (\Delta m^D / |\Delta m_{Max}^D| + \Delta m^M / |\Delta m_{Max}^M|) \cos(\theta_H)$ with $H_C^D = 3$ kOe, $\Delta J_D = 1\% H_C^D$, $H_C^M = 6$ kOe and $\Delta J_M = 1\% H_C^M$. It is shown also the best conditions to observe the maximum number of magneto-optical interactions.

4. Conclusion

The behavior of magneto-optical interactions in magnetic structures revealed two types of predominant magnetic states, i. e., demagnetized and magnetized. Understanding how each state arises due to the different effects produced during the magnetization process makes its study of fundamental importance for applications of devices in areas such as quantum computing and engineering. Our results also represent an efficient way to describe the behavior of magneto-optical interactions by directly considering the angular dependence of the interactions undergoing the magnetic field during the magnetization process. Furthermore, the results obtained show that the effects that cause global magnetic states to arise influence the excitation of spin waves. In terms of fundamentals, the

results show a significant advance in understanding the behavior of magneto-optical interactions in structures.

Acknowledgements

This research was supported by Conselho Nacional de Desenvolvimento Científico e Tecnológico (CNPq), Coordenação de Aperfeiçoamento de Pessoal de Nível Superior (CAPES), Financiadora de Estudos e Projetos (FINEP), Centro Multiusuário de Pesquisa e Caracterização de Materiais da Universidade Federal Rural de Pernambuco (CEMUPEC-UFRPE), and Fundação de Amparo à Ciência e Tecnologia do Estado de Pernambuco (FACEPE).

Conflicts of interest

The authors declare no conflicts of interest.

Data availability statement

Data underlying the results presented in this paper are not publicly available at this time but may be obtained from the authors upon reasonable request.

References

- [1] J. Holanda et al., Magnetic Damping Modulation in $\text{IrMn}_3/\text{Ni}_{80}\text{Fe}_{20}$ via the Magnetic Spin Hall effect, *Phys. Rev. Lett.* **124**, 087204 (2020).
- [2] J. Holanda, Analyzing the magnetic interactions in nanostructures that are candidates for applications in spintronics, *J. Phys. D: Appl. Phys.* **54**, 245004 (2021).
- [3] U. Cvelbar, Large-scale synthesis of nanowires, *J. Phys. D: Appl. Phys.* **44**, 174014 (2011).

- [4] L. Liu, Y. Diao, S. Xia, F. Lu, J. Tian, A first principle study on systematic stability and electronic properties of GaN nanowire surface with Cs/Li/NF₃ co-adsorption, **478**, 393 (2019).
- [5] Z. Lv, L. Liu, X. Zhangyang et al. Enhanced absorptive characteristics of GaN nanowires for ultraviolet (UV) photocathode. *Appl. Phys. A* **126**, 152 (2020).
- [6] C. A. França et al., Transmission electron microscopy as a realistic data source for the micromagnetic simulation of polycrystalline nickel nanowires, **128**, 42 (2017).
- [7] Y. Xiong, H. Luo, Y. Nie, F. Chen, W. Day, X. Wang, Y. Cheng, R. Gong., Synergistic effect of silica coated porous rodlike nickel ferrite and multi-walled carbon nanotube with improved electromagnetic wave absorption performance, *J. All. Comp.* **802**, 364 (2019).
- [8] P. Landeros et al., Reversal modes in magnetic nanotubes, *Appl. Phys. Lett.* **90**, 102501 (2007).
- [9] A. Mourachkine, O. V. Yazyev, C. Ducat, J.-Ph Ansermet, Template nanowires for spintronics applications: nanomagnet microwave resonators functioning in zero applied magnetic field, *Nano Lett.* **8**, 3683 (2008).
- [10] O. Yalçın et al., A comparison of the magnetic properties of Ni and Co nanowires deposited in different templates and on different substrates, *J. Magn. Magn. Mater.*, **373**, 207 (2015).
- [11] C. Bran, A. P. Espejo, E. M. Palmero, J. Escrig, M. Vázquez, Angular dependence of coercivity with temperature in Co-based nanowires, *J. Magn. Magn. Mater.*, **396**, 327 (2015).
- [12] S. C. Sepúlveda, R. M. Corona, D. Altbir, J. Escrig, Magnetic properties of mosaic nanocomposites composed of nickel and cobalt nanowires, *J. Magn. Magn. Mater.*, **416**, 325 (2016).

- [13] J. Holanda, D. B. O. Silva, E. P. Hernández, Angular dependence of the coercivity in arrays of ferromagnetic nanowires, *J. Magn. Magn. Mater.*, **378**, 228 (2015).
- [14] N. Zafar et al., Effects of pH on the crystallographic structure and magnetic properties of electrodeposited cobalt nanowires, *J. Magn. Magn. Mater.*, **377**, 215 (2015).
- [15] C. Bran et al., Direct observation of transverse and vortex metastable magnetic domains in cylindrical nanowires, *Phys. Rev. B* **96**, 125415 (2017).
- [16] J. García et al., Magnetization reversal dependence on effective magnetic anisotropy in electroplated Co–Cu nanowire arrays, *J. Mater. Chem. C* **3**, 4688 (2015).
- [17] E. C. Stoner and E. P. Wohlfarth, Generalized Stoner-Wohlfarth model and the non-langevin magnetism of single-domain particles, *Philos. Trans. R. Soc. London, Ser A* **240**, 599 (1948).
- [18] A. Aharoni and S. Shtrikman, Magnetization curve of the infinite cylinder, *Physical Review* **109**, 5 (1958).
- [19] A. Aharoni, Angular dependence of nucleation by curling in a prolate spheroid, *J. Appl. Phys.* **82**, 1281 (1997).
- [20] R. Lavín et al., Angular dependence of magnetic properties in Ni nanowire arrays, *J. Appl. Phys.* **106**, 103903 (2009).
- [21] J. Dong et al., Influence of tensile stress on giant magnetoimpedance effect of electroplated $Ni_{1-x}Co_x/Cu$ composite wires, *J. All. Comp.* **616**, 426 (2014).
- [22] O. Henkel, Remanenzverhalten und wechselwirkungen in hartmagnetischen teilchenkollektiven, *Status Solidi* **7**, 919 (1964).
- [23] P. E. Kelly, K. O'Gray, P. I. Mayo, R. W. Chantrell, Switching mechanisms in cobalt-phosphorus thin films, *IEEE Trans. Magn.* **25**, 3881 (1989).

- [24] I. Klik and Y. D. Yao and C. R. Chang, Henkel plots for thermally relaxing systems, *J. Appl. Phys.* **81**, 5230 (1997).
- [25] P. I. Mayo, K. O'Grady, P. E. Kelly, and J. Cambridge, I. L. Sanders and T. Yogi, R. W. Chantrell, A magnetic evaluation of interaction and noise characteristics of CoNiCr thin films, *J. Appl. Phys.* **69**, 4733 (1991).
- [26] C. J. Buehler and I. D. Mayergoyz, Henkel plots and the Preisach model of hysteresis, *J. Appl. Phys.* **79**, 5746 (1996).
- [27] E. P. Wohlfarth, Relations between Different Modes of Acquisition of the Remanent Magnetization of Ferromagnetic Particles, *J. Appl. Phys.* **29**, 595 (1958).
- [28] M. Grimsditch, Y. Jaccard, and Ivan K. Schuller, Magnetic anisotropies in dot arrays: Shape anisotropy versus coupling, *Phys. Rev. B* **58**, 11539 (1998).
- [29] A. Encinas-Oropesa, M. Demand, L. Piraux, I. Huynen and U. Ebels, Dipolar interactions in arrays of nickel nanowires studied by ferromagnetic resonance, *Phys. Rev. B* **63**, 105515 (2001).
- [30] S. M. Rezende and F. R. Morgenthaler, Magnetoelastic waves in time-varying magnetic fields. I. Theory, *J. Appl. Phys.* **40**, 524 (1969).
- [31] Z. Zhang et al., Spin-wave frequency division multiplexing in an yttrium iron garnet microstripe magnetized by inhomogeneous field, *Appl. Phys. Lett.* **115** (23), 232402 (2019).
- [32] J. Holanda, D. S. Maior, A. Azevedo, and S. M. Rezende, Detecting the phonon spin in magnon-phonon conversion experiments, *Nat. Phys.* **14**, 500 (2018).
- [33] S. M. Rezende, D. S. Maior, O. Alves Santos, and José Holanda. Theory for phonon pumping by magnonic spin currents. *Phys. Rev. B* **103**, 144430 (2021).

- [34] S. M. Rezende, Fundamentals of Magnonics, Lecture Notes in Physics Vol. 969 (Springer, Cham, Switzerland, 2020).